



Contents lists available at ScienceDirect

European Journal of Medicinal Chemistry

journal homepage: <http://www.elsevier.com/locate/ejmech>

Research paper

Novel benzenesulfonamide and 1,2-benzisothiazol-3(2H)-one-1,1-dioxide derivatives as potential selective COX-2 inhibitors

Ehab S. Taher^{a,*}, Tarek S. Ibrahim^{b,c}, Mohamed Fares^{d,e}, Amany M.M. AL-Mahmoudy^c, Abdullah F. Radwan^f, Khaled Y. Orabi^g, Osama I. El-Sabbagh^{h,i}^a Pharmaceutical Organic Chemistry Department, Faculty of Pharmacy, Al-Azhar University, 71524, Assiut, Egypt^b Pharmaceutical Chemistry Department, Faculty of Pharmacy, King Abdulaziz University, 21589, Saudi Arabia^c Pharmaceutical Organic Chemistry Department Faculty of Pharmacy, Zagazig University, Zagazig, 44519, Egypt^d School of Chemistry, University of Wollongong, Wollongong, 2522, NSW, Australia^e School of Chemistry, The University of Sydney, 2006, NSW, Australia^f Biochemistry Department, Faculty of Pharmacy, Egyptian Russian University, 11829, Cairo, Egypt^g Department of Pharmaceutical Chemistry, Faculty of Pharmacy, Health Sciences Center, Kuwait University, 13110, Safat, Kuwait^h Pharmaceutical Chemistry Department, Faculty of Pharmacy, Taif University, 11099, Taif, Saudi Arabiaⁱ Medicinal Chemistry Department, Faculty of Pharmacy, Zagazig University, 44519, Zagazig, Egypt

ARTICLE INFO

Article history:

Received 15 December 2018

Received in revised form

1 March 2019

Accepted 16 March 2019

Available online 20 March 2019

Keywords:

Anti-inflammatory

COX-2

Benzenesulfonamide

Benzisothiazol

Saccharin

Celecoxib

ABSTRACT

Two new series of 1,2-benzisothiazol-3(2H)-one-1,1-dioxide derivatives containing either five membered heterocyclic rings or aryl hydrazones were synthesized and evaluated for their *in vitro* COX-1/COX-2 inhibitory activity. *In vivo* anti-inflammatory evaluation revealed that benzenesulfonamides bearing pyrazole moiety **19**, **20** and its cyclized form **23** exhibited the highest anti-inflammatory activity with comparable potency to celecoxib. Furthermore, the ulcerogenic activity evaluation showed that compounds **19**, **20** and **23** exerted the minimal ulcer index in comparison to indomethacin as a reference drug. Docking studies of the most selective COX-2 derivatives were also carried out against COX-2 active site. Benzenesulfonamide derivatives **19** and **20** displayed higher predicted binding affinities inside the COX-2 active site. Molecular modelling simulation and drug likeness studies showed good agreement with the obtained biological evaluation.

Crown Copyright © 2019 Published by Elsevier Masson SAS. All rights reserved.

1. Introduction

Non-steroidal anti-inflammatory drugs (NSAIDs) are one of the most widely prescribed and cost-effective drugs for pain relief. They represent approximately 5–10% of all medications prescribed each year [1]. These medications inhibit the cyclooxygenase enzymes (COX-1 and COX-2), which are responsible for arachidonic acid metabolism to prostaglandin H₂ (PGH₂), the precursor for prostacyclin (PGI₂), prostaglandin-E₂ (PGE₂) and thromboxane-A₂ (TXA₂) synthesis [2]. Chronic use of NSAIDs has been implicated in severe gastric ulcers and renal disorders [3] due to inhibition of COX-1. These side effects of the traditional NSAIDs are the main reason for drug intolerance and discontinuation [4]. Previous studies

succeeded in the synthesis of new NSAIDs as selective COX-2 inhibitors, namely “coxibs” to minimize the danger of gastric ulcers [5], however the cardiovascular adverse effects were significant [6–8]. Within the coxibs class of drugs, Celecoxib has the advantage of lowering cardiovascular toxicity compared to other coxibs [9].

Various attempts for safer NSAIDs have been made in the last few years, through optimization of benzenesulfonamide-based derivatives, considering celecoxib **1**, bearing a pyrazole ring linked to benzenesulfonamide ring at *N*-1 and *p*-tolyl group at *C*-5, as a lead compound (Fig. 1) [10].

Saccharin **2** has played a crucial role in the development of several biologically active agents such as repinotan, supindimide and ipsapirone [11]. Meanwhile, piroxicam **3**, the lead compound of oxicams NSAIDs family (Fig. 1), was discovered as a saccharin derivative through utilizing the Gabriel–Colman rearrangement under basic conditions [12].

The varied functionality associated with sodium saccharin, as a useful chiron, has promoted many attempts for synthesis of a wide

* Corresponding author. Lecturer of Pharmaceutical Organic chemistry at the Department of Pharmaceutical Organic Chemistry, Faculty of Pharmacy, Al-Azhar University, 71524, Assiut, Egypt.

E-mail address: ehabtaher@azhar.edu.eg (E.S. Taher).

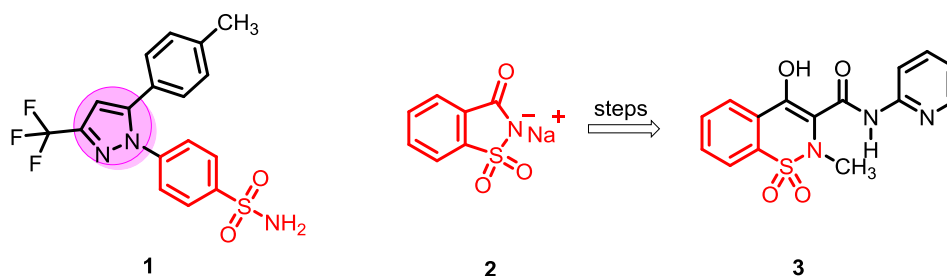


Fig. 1. Structure of celecoxib **1**, sodium saccharin **2** and piroxicam **3**.

range of benzenesulfonamides. Several studies have investigated the analgesic and anti-inflammatory activities of the benzenesulfonamides scaffold attached to a pyrazole moiety [13]. For instance, compounds **4** and **5** possessed higher analgesic and anti-inflammatory activities than celecoxib [13,14]. In addition, it was reported that 1,5-diphenyl pyrazoles exhibited anti-inflammatory activities less than diclofenac against COX-1 but they showed a reasonable *in vitro* COX-2 inhibitory activity with IC₅₀ value of 0.45 μ M [15]. Likewise, compounds **6** displayed high COX-2 selectivity and high anti-inflammatory activity compared to celecoxib [16]. Celecoxib derivative **7** was found to have higher anti-inflammatory activity and COX-2 selectivity with reasonable ulcer index [17]. The pyrazolyl benzenesulfonamides linked to thiazolidinone **8** and pyrazole **9** displayed higher COX-2 selectivity with minimal potential for gastric injury (Fig. 2) [18].

In our ongoing investigation of the structure activity relationship of benzenesulfonamide anti-inflammatory activity, we designed and synthesized a novel set of benzenesulfonamide derivatives starting from commercially available sodium saccharin. The pivotal features of our approach aimed to do some structural variations on celecoxib skeleton to explore the shifting effect of pyrazole ring located at *para*-position of the benzenesulfonamide moiety as seen in celecoxib to *ortho*-position, as in our targets **19** and **20** on not only COX-2 selectivity but also to explore the new possible receptor interactions. Moreover, the effect of replacement of the *ortho* pyrazole ring with its bioisosteres, such as, 1,3,4-oxadiazole i.e. **12** and **13** and triazole, i.e. **15** and **16** was also considered. Another focus of our investigation was rigidification of the benzenesulfonamide moiety, by ring closure towards the

dipyrazole derivative **23**, to adopt a preferred binding conformation to COX-2 and reduce the entropic loss, which might enhance the potency and efficacy as well.

2. Discussion

2.1. Chemistry

In this work, novel series of acyclic benzenesulfonamide derivatives bearing 1,3,4-oxadiazole or triazole moieties were prepared as shown in Schemes 1 and 2. *N*-alkyl saccharins **10**, **17** and **21** were prepared *via* the reaction of benzyl bromide, isopropyl iodide and diethyl bromomalonate respectively, with sodium saccharin by heating the reactants in dimethylformamide (DMF) for 2 h [19]. The key hydrazide intermediates **11**, **18** and **22** were prepared by stirring *N*-benzyl, *N*-isopropyl saccharins or its diester derivative **10**, **17** and **21**, respectively with excess hydrazine hydrate at room temperature for 15–20 min following the reported procedure [13]. The hydrazide **11** was cyclized through its reaction with carbon disulfide in basic condition to afford the targeted 1,3,4-oxadiazole bioisoster **12** in high yield (70%). Subsequent alkylation of oxadiazole **12** with benzyl bromide and ethyl iodide in ethanol containing potassium hydroxide at room temperature gave the desired novel thioalkylated derivatives **13a** and **13b**, respectively.

In addition, the aminotriazole bioisostere **15** was synthesized *via* heating the intermediate **14** at reflux with hydrazine hydrate. The set of hydrazones **16a–d** were then prepared through condensation of aminotriazole **15** with appropriate aromatic aldehydes through heating at reflux in acetic acid for 20 min.

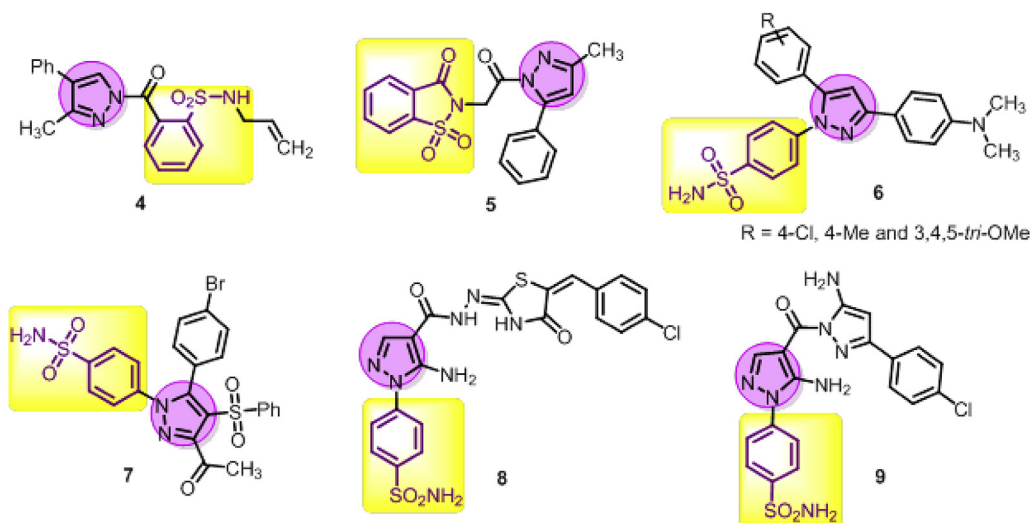
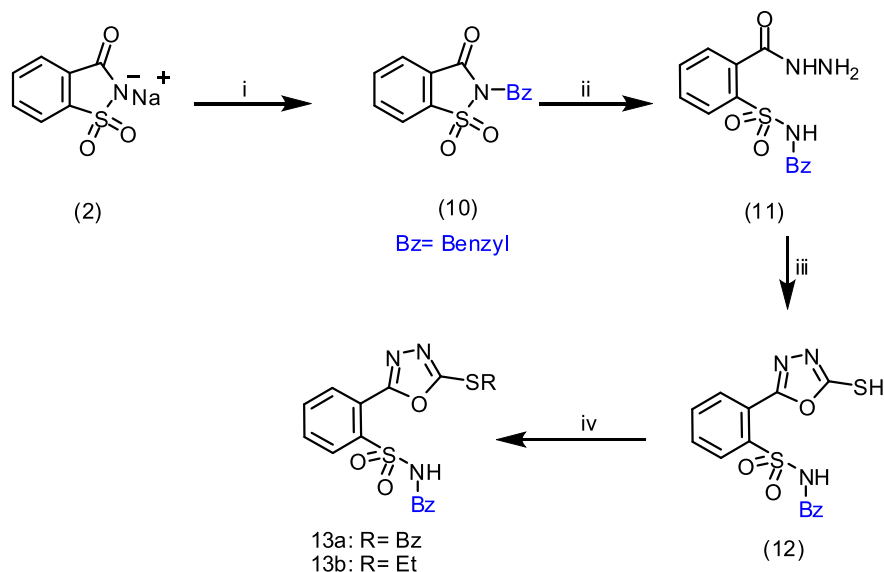
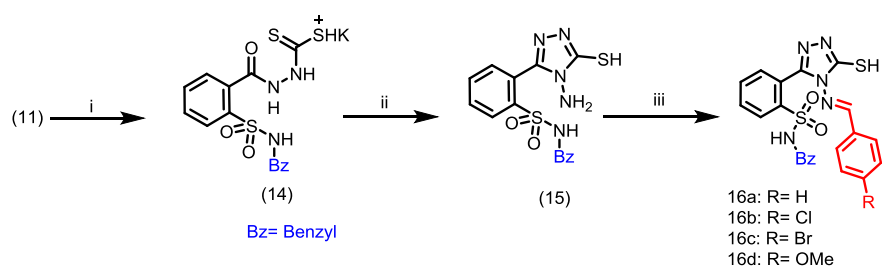


Fig. 2. Literature survey for benzenesulfonamide derivatives with anti-inflammatory and analgesic activities.



Scheme 1. Reagents and conditions: (i) benzyl bromide, DMF, reflux, 2 h; (ii) NH_2NH_2 , r.t, 15 min; (iii) CS_2 , KOH, EtOH, reflux, 6 h; (iv) benzyl bromide and or ethyl iodide, EtOH, KOH, r.t, 2 h.



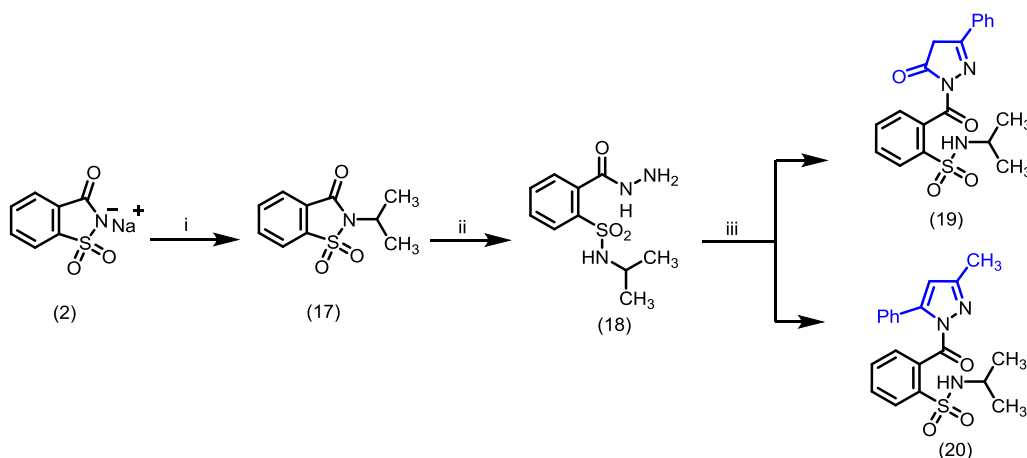
Scheme 2. Reagents and conditions: (i) EtOH, CS_2 , KOH, r.t, 14 h; (ii) NH_2NH_2 , reflux, 1 h; (iii) Ar-CHO, AcOH, reflux, 20 min.

New pyrazoles **19**, **20**, **23** and dihydrazones derivatives **24a-c** were synthesized as shown in Schemes 3 and 4. The hydrazides **18** and **22** were cyclized with β -diketones; namely benzoylacetate and benzoylacetone; *via* heating equimolar amounts of the reactants under reflux in ethanol containing catalytic amount of acetic acid for 12 h to afford the novel pyrazole derivatives **19**, **20** and **23** in higher yields, 80%, 85% and 75%, respectively.

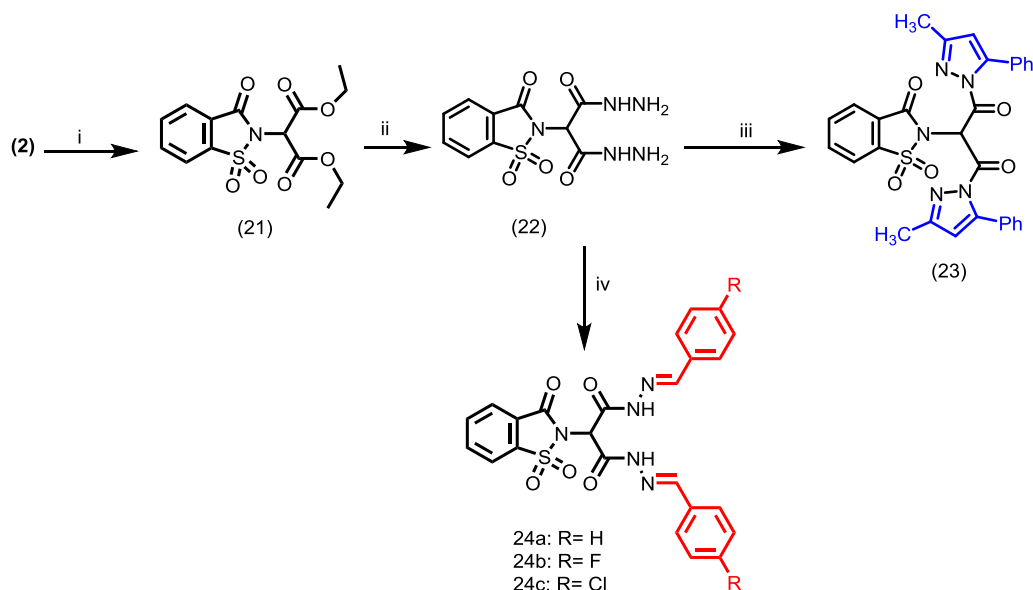
In a related vein, the dihydrazide **22** was condensed with

appropriate aromatic aldehydes *via* heating the reactants in ethanol containing catalytic amounts of glacial acetic acid to give the anticipated novel dihydrazone derivatives **24a-c**.

The novel benzenesulfonamide derivatives were characterized by using thin layer chromatography and melting points techniques. Structures of novel compounds were determined using elemental analyses, IR, ^1H NMR, ^{13}C NMR and mass spectroscopic methods.



Scheme 3. Reagents and conditions: (i) Isopropyl iodide, DMF, reflux, 2 h; (ii) NH_2NH_2 , r.t, 2 h; (iii) benzoylacetate and/or benzoylacetone, EtOH, AcOH, reflux, 12 h.



Scheme 4. Reagents and conditions: (i) diethyl 2-bromomalonate, DMF, reflux, 2 h; (ii) NH_2NH_2 , r.t, 20min; (iii) benzoyl acetone, EtOH, AcOH, reflux, 12 h; (iv) Ar-CHO, EtOH, AcOH reflux, 2 h.

2.2. Biology

2.2.1. *In vitro* COX-1/COX-2 enzyme inhibition assay

All the compounds were tested for their *in vitro* COX-1 and COX-2 inhibitory effect as depicted in Table 1 [20]. The efficacies of tested compounds were measured as the concentration causing 50% enzyme inhibition (IC_{50}) as shown in Table 1, while selectivity indices (SI values) defined as IC_{50} (COX-1)/ IC_{50} (COX-2) were calculated and then compared to the selective COX-2 inhibitor, celecoxib. The results indicated the tested compounds have strong to fair COX-1 inhibition (IC_{50} : 1.98–12.23 μM), in comparison to celecoxib (IC_{50} : 14.8 μM).

The structure activity data acquired suggested that installing the oxadiazole pharmacophore into the benzenesulfonamide as seen in compound **12** caused a weak inhibition of COX-2 (IC_{50} : 0.52 μM) while its alkylated derivative **13a** bearing benzyl group (IC_{50} :

0.39 μM) showed slight improvement in activity but its ethyl derivative **13b** (IC_{50} : 0.71 μM) was less effective. This improvement in activity may be due to increasing the bulkiness of oxadiazole ring. In general, oxadiazole ring and its alkylated derivatives showed weak inhibition of COX-2 (IC_{50} : 0.39–0.71 μM) in comparison with celecoxib as a reference drug (IC_{50} : 0.05 μM) and therefore, the oxadiazole ring is not preferable for COX-2 inhibitory effect. It was noted however, that replacement of oxadiazole ring with a triazole as seen in compound **15** (Table 1) enhanced COX-2 inhibition activity (IC_{50} = 0.23 μM).

The introduction of bulky groups on the free amino group of the triazole moiety (**15**) through hydrazone formation (**16a–d**) caused a decrease for both COX-2 activity (IC_{50} : 0.38–0.65 μM , Table 1) and selectivity (SI = 6.9–12.2) in comparison with celecoxib (IC_{50} : 0.05 μM , SI = 296). It was noted that the free amino group may assist binding on the COX-2 active site. Hence, it is proposed benzenesulfonamides bearing the *ortho*-triazole ring (**15**) is preferential over the oxadiazole (**12**) for COX-2 inhibitory activity.

Conversely, a remarkable improvement in COX-2 inhibitory activity as well as selectivity was observed upon replacement of the five membered triazole ring with pyrazole as seen in compound **19**, (IC_{50} 0.09 μM , SI = 135.9) and compound **20** (IC_{50} = 0.06 μM , SI = 154.0). Introduction of an extra pyrazole ring to the cyclized benzenesulfonamide skeleton (compound **23**) caused marked increase of both COX-2 potency and selectivity (IC_{50} = 0.05 μM , SI = 236) which is comparable to celecoxib (IC_{50} : 0.05 μM , SI = 296). Considering structural modification of the later compound through replacement of the di-pyrazole rings with dihydrazone moieties (**24a–c**) led to a deleterious effect on both COX-2 potency and selectivity (Table 1). It was noted that benzenesulfonamide derivatives bearing pyrazole or dipyrazole 5-membered rings showed higher COX-2 inhibitory activity and selectivity than their corresponding dihydrazone ones. This may contribute to the molecule's ability to be engaged in intermolecular interactions with COX-2 active site. The order of activity of 5-membered rings towards COX-2 inhibitory activity is cyclized benzenesulfonamide bearing dipyrazole > pyrazole > triazole > oxadiazole.

In conclusion, among tested compounds, benzenesulfonamides bearing pyrazole ring **19** and **20** showed high activity against COX-2 with IC_{50} : 0.09 (SI = 135.9), 0.06 μM (SI = 154), respectively, while

Table 1
Data of the *in vitro* COX-1/COX-2 enzyme inhibition assay of the designed compounds.

Compounds	IC_{50} (μM) ^a		SI ^b
	COX-1	COX-2	
12	4.52	0.52	8.70
13a	3.68	0.39	9.40
13b	8.21	0.71	11.60
15	2.98	0.23	13.00
16a	6.45	0.53	12.20
16b	5.71	0.65	8.80
16c	4.21	0.38	11.00
16d	3.25	0.47	6.90
19	12.23	0.09	135.90
20	9.24	0.06	154.00
23	11.81	0.05	236.20
24a	1.98	0.29	6.80
24b	2.78	0.12	23.20
24c	7.65	0.61	12.50
Celecoxib	14.8	0.05	296.00

^a IC_{50} value is the compound concentration required to produce 50% inhibition of COX-1 or COX-2 for means of two determinations and deviation from the mean is <10% of the mean value.

^b SI: Selectivity index IC_{50} (COX-1)/ IC_{50} (COX-2).

cyclized benzenesulfonamide bearing dipyrazole rings **23** (IC₅₀: 0.05 μM, SI = 236) was the most potent, with a comparable activity to celecoxib (IC₅₀: 0.05 μM, SI = 296.00), thus, these compounds (**19**, **20** and **23**) can be considered as improved drug leads as opposed to celecoxib.

2.2.2. *In vivo* anti-inflammatory evaluation and ulcerogenic liability

The novel benzenesulfonamide derivatives **15**, **19**, **20**, **23** and **24b**, which showed the highest *in vitro* COX-2 inhibitory activity, were selected to evaluate their *in vivo* anti-inflammatory and ulcerogenic activities.

2.2.2.1. Anti-inflammatory effect evaluation. Anti-inflammatory activity was evaluated by employing the carrageenan rat hind paw edema method using celecoxib as a reference drug [21]. Mean changes in paw edema thickness after 1, 2, 3 and 4 h from induction of inflammation and percentages of edema inhibition given by the tested compounds and celecoxib at 18 mg/kg body weight dose level are displayed in Table 2.

It was noted that all the tested compounds displayed a very similar figure regarding anti-inflammatory activity which ranges from 49.19 to 65.32% reduction in inflammation after 4 h in comparison to celecoxib (62.90% reduction in inflammation after 4 h).

The benzenesulfonamide derivative bearing triazole ring **15** which showed a very weak *in vitro* COX-2 inhibitory activity, had the lowest anti-inflammatory activity with edema inhibition % = 39.73 after 1 h to 49.19 after 4 h.

In contrast, benzenesulfonamide derivatives bearing pyrazole ring **19**, **20** and the cyclized dipyrazole form **23** which exhibited potent *in vitro* COX-2 inhibitory activity and selectivity (Table 1) had high anti-inflammatory activity (edema inhibition % = 56.45, 65.32, 61.29, respectively after 4 h).

Unexpectedly, the benzenesulfonamide derivative bearing dihydrazone **24b**, which exhibited a weak *in vitro* COX-2 inhibitory activity, showed a high anti-inflammatory effect (edema inhibition % = 54.26 after 4 h).

The higher *in vivo* potency of pyrazole motifs **19**, **20** and **23** might reflect their better pharmacokinetic properties and higher systemic bioavailability. This might be partly due to their enhanced aqueous solubility and thereby, increased rate of dissolution through different biological membranes. In conclusion, a

correlation between *in vitro* selective COX-2 inhibition and *in vivo* anti-inflammatory effect was established.

2.2.2.2. Ulcerogenic liability. The ulcerogenic activity for the selected derivatives was determined at 18 mg/kg body weight dose level using celecoxib and indomethacin as reference drugs [22].

The data obtained from Table 3 revealed that benzenesulfonamide with triazole **15** and dihydrazone **24b** can cause stomach ulceration (ulcer index: **15**: 360; and **24b**: 120) in comparison with both the selective COX-2 inhibitor celecoxib (ulcer index: 3) and indomethacin as ulcerogenic drug (ulcer index: 480) and these results agree with *in vitro* COX-2 inhibitory activity. A remarkable and nearly equipotent effect to celecoxib (ulcer index: 3) was observed for benzenesulfonamide carrying pyrazole ring **19**, **20** and its cyclized derivative bearing dipyrazole rings **23** (ulcer index: 4).

Therefore, the pivotal anti-inflammatory value of these compounds **19**, **20** and **23** is that they possess significantly improved safety margin on gastric mucosa than indomethacin. These positive results supported the aim of our protocol to develop a novel series of benzenesulfonamide derivatives as COX-2 inhibitors with minimal gastrointestinal side effects.

2.2.3. Molecular docking

The inhibitory profiles of celecoxib and the compounds **19**, **20** and **23** (Table 1) were further studied by docking into the COX-2 active site (PDB code: 3ln1) to gain insight into the potential binding modes [23]. Celecoxib exploited the side pocket near Val523 in COX-2 (which is not present in COX-1) and inserted its phenyl sulfonamide part into it. The sulfonamide NH₂ forms three hydrogen bonds with the hydrophilic side chains of Ser339 and Gln178 in the side pocket and the carbonyl group at residue Leu338. The *p*-tolyl and the trifluoromethyl methyl moieties of the celecoxib occupied hydrophobic regions in the active site (Fig. 3).

By a careful analysis of the docked poses of compounds **19**, **20** and **23**, it was clear that both compound **19** and **20** can occupy the same pocket as celecoxib, but compound **23** could not, likely due to its bulkiness. While the predominant binding site nature of COX enzymes is hydrophobic, hydrophilic amino acids residues were found in the side pocket of COX-2, including Ser339, Tyr341, Tyr371, Arg499 and Ser516. The sulfone in compound **19** was observed to be capable of forming a hydrogen bond with the Tyr341 of the COX-2 active site (Fig. 3). The sulfonamide group was surrounded by

Table 2
Anti-inflammatory activity of the tested compounds and Celecoxib (18 mg/kg p.o.) against formalin-induced paw edema in rats. (Mean ± S.D; n = 6).

Treatment	Initial thickness	Rat paw thickness (mm)			
	Zero time	1 h	2 h	3 h	4 h
Control	0.24 ± .024	0.73 ± 0.03	0.84 ± 0.02	0.94 ± 0.02	1.24 ± 0.02
Celecoxib	0.24 ± .024	0.41 ± 0.02 ^a	0.44 ± 0.01 ^a	0.44 ± 0.03 ^a	0.46 ± 0.03 ^a
15	0.24 ± .024	0.44 ± 0.02 ^a	0.48 ± 0.01 ^a	0.56 ± 0.02 ^{a,b}	0.63 ± 0.02 ^{a,b}
19	0.24 ± .024	0.42 ± 0.01 ^a	0.50 ± 0.02 ^a	0.52 ± 0.02 ^a	0.54 ± 0.01 ^a
20	0.24 ± .024	0.32 ± 0.02 ^a	0.36 ± 0.01 ^a	0.38 ± 0.03 ^a	0.43 ± 0.03 ^a
23	0.24 ± .024	0.36 ± 0.02 ^a	0.41 ± 0.01 ^a	0.41 ± .029 ^a	0.48 ± 0.01 ^a
24b	0.24 ± .024	0.36 ± 0.01 ^a	0.40 ± 0.02 ^a	0.43 ± 0.01 ^a	0.55 ± 0.01 ^a
Treatment	Edema inhibition %				
		1 h	2 h	3 h	4 h
Control	-----	0	0	0	0
Celecoxib	-----	43.84	47.62	53.19	62.90
15	-----	39.73	42.86	45.43	49.19
19	-----	42.47	43.48	44.68	56.45
20	-----	56.17	57.14	59.58	65.32
23	-----	50.69	51.19	56.38	61.29
24b	-----	50.69	52.38	54.25	54.26

^a Significantly different from normal control at p < 0.05.

^b Significantly different from Celecoxib at p < 0.05 within the same column.

Table 3Ulcerogenic effect of Celecoxib, **15**, **19**, **20**, **23** and **24b** (18 mg/kg) in rats and Indomethacin (18 mg/kg). (Mean \pm S.D, n = 6).

Treatment	Average severity (ulcer score)	% Incidence of gastric ulceration	Ulcer index
Control	0.00 \pm 0.00	0	0
Celecoxib	0.00 \pm 0.00	0	3
Indomethacin	4.80 \pm 0.20 ^{a,b}	100	480
15	3.60 \pm 0.24 ^{a,b,c}	100	360
19	0.20 \pm 0.20 ^c	20	4
20	0.20 \pm 0.20 ^c	20	4
23	0.20 \pm 0.20 ^c	20	4
24b	1.20 \pm 0.20 ^{a,b,c}	100	120

^a Significantly different from normal control at $p < 0.05$.^b Significantly different from Celecoxib at $p < 0.05$.^c Significantly different from Indomethacin at $p < 0.05$.

basic residues Arg499 and His75 in case of compound **19** and His75 in the case of compound **20**. Van der Waals interactions with Val335, Leu338, Ala513 and Val509 dominate the remainder of the compound **20** and **23** interactions. Overlaying of celecoxib and compound **20** illustrated they possess a similar active conformation of the trifluoropyrazole and the *p*-tolyl of celecoxib with the 5-methylpyrazole and the phenyl in compound **20**, respectively (Fig. 3). However, celecoxib phenyl sulfonamide was perpendicular on its congener in compound **20**, possibly due to the presence of the carbonyl group between the phenyl sulphonamide and the pyrazole moiety in compound **20**.

Compound **23** binds to the exposed part of the receptor, presumably due to its bulky size (Fig. 4). Clusters of hydrophilic amino acids, including three basic residues His80, His75 and His337 were found in the pocket. The phenyl group in 3-oxobenzod[*d*]isothiazole and the methyl group of the pyrazole moiety formed a pi-pi hydrophobic interaction with Pro500 and Pro177, respectively.

In general, data obtained from docking studies showed that compounds **19** and **20** can occupy the binding site of the enzyme

with binding interaction energy ranging from -10.6 kcal/mol to -11.3 kcal/mol relative to celecoxib -13.8 kcal/mol. Compound **23** binds to an exposed pocket of COX-2 with a binding energy -6.3 kcal/mol.

2.2.4. Pharmacokinetic properties and drug likeness

The drug likeness, HBD and HBA scores of the most active compounds **15**, **19**, **20**, **23**, **24b** were calculated using the MolSoft online calculation kits [24]. Prediction of the lipophilicity was performed using ALOGPS 2.1 program 5, while calculation of TPSA, the number of rotatable bonds, used the Molinspiration property calculation kit 6. The compounds have 5 rotatable bonds except **24b** has 7 rotatable bonds (Table 4). Reduced molecular flexibility is measured by the number of rotatable bonds and is greatly linked to oral bioavailability [25]. The number of rotatable bonds less or equal to ten potentially increases the oral bioavailability [26]. Topological polar surface area (TPSA), for these five compounds, with range from 81.07 to 137.38, is a very valuable parameter for the prediction of drug transport properties and oral bioavailability. The

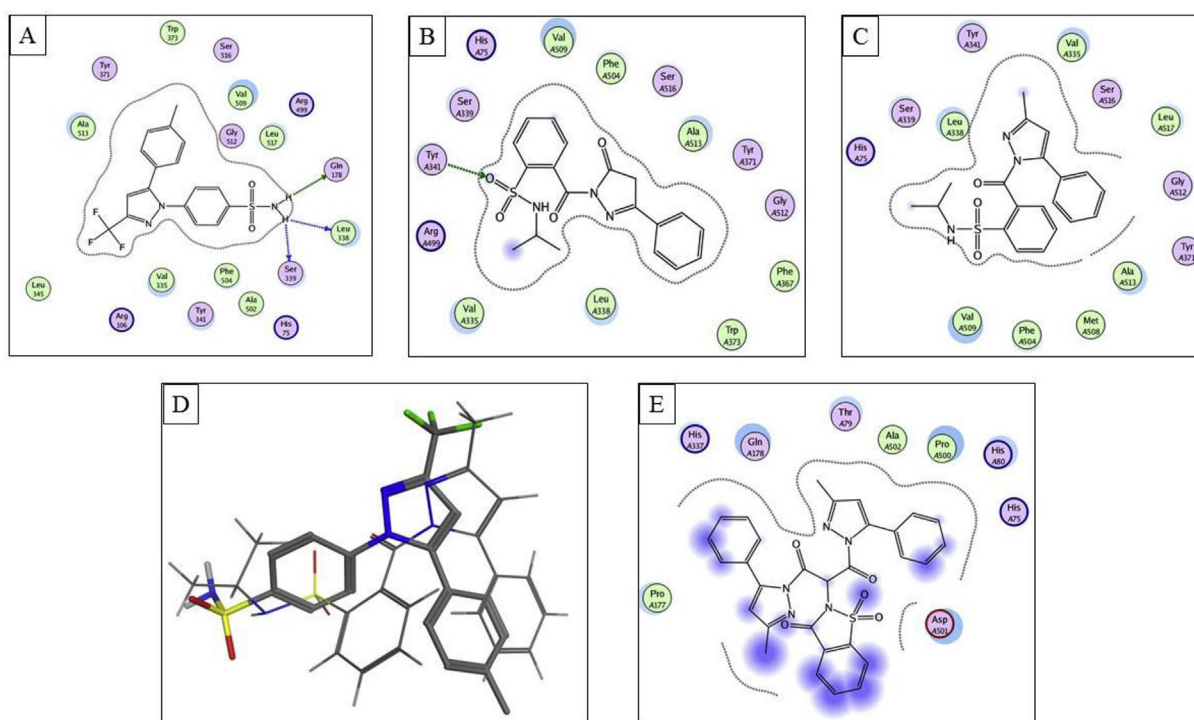


Fig. 3. 2D representations of the proposed binding patterns of celecoxib (A), **19** (B), **20** (C) and **23** (E) into the cyclooxygenase 2 (PDB code 3ln1) and overlaying of celecoxib and compound **20** (D).

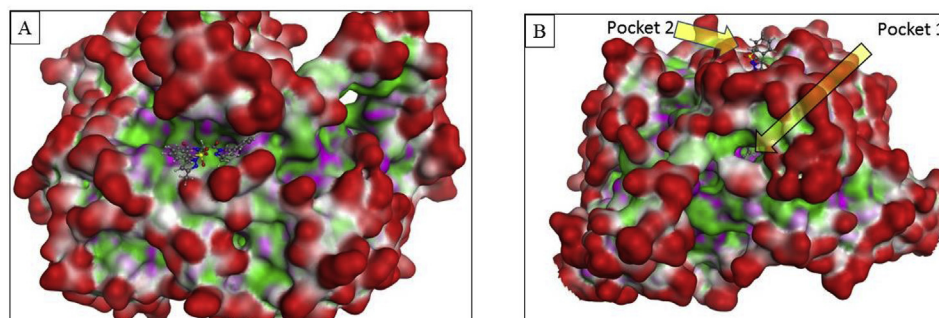


Fig. 4. Representations of the docked compound **23** into the cyclooxygenase 2 (PDB code 3ln1) (A) and representation of the two binding pockets identified in the COX-2, where pocket 1 (active site) is occupied by celecoxib, compounds **19** and **20** and the exposed pocket 2 occupied by compound **23** (B). Pink: polar; green: hydrophobic; red: exposed. (For interpretation of the references to color in this figure legend, the reader is referred to the Web version of this article.)

Table 4

Drug likeness calculations and Lipinski parameters of the compounds 15, 19, 20, 23 and 24b.

	M. Wt ^a	log P ^b	HBA ^c	HBD ^d	n violations ^e	n _{rot} ^f	TPSA ^g	Volume ^h	DLS
15	361.45	2.15	6	4	0	5	102.91	293.50	−0.58
19	385.44	2.10	6	1	0	5	95.91	329.21	−0.34
20	383.47	3.26	5	1	0	5	81.07	337.40	−0.64
23	565.61	4.49	7	0	1	5	124.25	472.37	0.26
24b	525.49	2.72	7	2	1	7	137.38	415.20	1.07

^a Molecular weight.

^b Lipophilicity.

^c Number of hydrogen bond acceptors.

^d Number of hydrogen bond donors.

^e Number of violations.

^f Number of rotatable bonds.

^g Topological polar surface area.

^h Molecular volume. DLS, Drug likeness score.

drug likeness score (DLS) of all these compounds was from −0.64 to 1.07 (Table 4). The dipyrazolyl **23** and dihydrazone **24b** benzenesulfonamide counterparts possessed maximum drug-likeness score of 0.26 and 1.07, respectively (Table 4).

Our physicochemical calculation indicated that these compounds fulfilled the Lipinski guidelines and have drug-likeness scores, which enables them to be potential oral bioavailable drugs.

3. Conclusion

Two new series, namely, benzenesulfonamide and 1,2-benzisothiazol-3(2H)-one-1,1-dioxide derivatives were synthesized using sodium saccharin as cheapest starting synthon. *In vitro* COX-2 inhibitory activity study revealed that benzenesulfonamides bearing pyrazole ring **19** and **20** showed high activity against COX-2 with IC₅₀: 0.09 (SI = 135.9) and 0.06 μM (SI = 154), respectively, meanwhile the cyclized benzenesulfonamide bearing dipyrazole rings **23** (IC₅₀: 0.05 μM, SI = 236) was the most potent, with a comparable activity to celecoxib (IC₅₀: 0.05 μM, SI = 296.0).

Moreover, anti-inflammatory activity and ulcer liability evaluation demonstrated compounds **19**, **20** and **23** possessed significant anti-inflammatory activity with low gastric ulceration which was comparable to celecoxib. Docking study showed that compounds **19** and **20** can occupy the binding site of the enzyme with binding interaction energy ranging from −10.6 kcal/mol to −11.3 kcal/mol compared to celecoxib −13.8 kcal/mol. Compound **23** binds to an exposed pocket of COX-2 with binding energy −6.3 kcal/mol. The obtained results from the *in silico* pharmacokinetic properties calculation, for compounds **19**, **20** and **23**, suggested that these compounds could be promising leads for further investigation to explore more about the structure inhibitor relationship and develop novel selective COX-2 inhibitors agent.

4. Experimental

4.1. Chemistry

Melting points were determined with a Gallenkamp (London, U.K.) melting point apparatus and are uncorrected. IR spectra (KBr, cm^{−1}) were recorded on Bruker Vector, 22FT-IR [Fourier Transform Infrared (FTIR), Germany] spectrometer. ¹H NMR and ¹³C NMR spectra were recorded on a Varian Gemini-200 (200 MHz, Foster City, Calif., USA), 400 and 600 spectrometers using dimethylsulphoxide DMSO/D₂O as a solvent and tetramethylsilane (TMS) as an internal standard (chemical shift in δ, ppm). Mass spectra were determined using Mass spectrometer GC/MS Shimadzu QP 1000 EX (Shimadzu Corporation, Tokyo, Japan) with ionization energy 70 eV. Elemental analyses were determined using Manual Elemental Analyzer Heraeus (Germany) and Automatic Elemental Analyzer CHN Model 2400 Perkin Elmer (USA) at Microanalytical Center, Faculty of Science, Cairo University, Egypt. All the results of elemental analyses corresponded to the calculated values within experimental error. Progress of the reaction was monitored by thin-layer chromatography (TLC) using precoated TLC sheets with Ultraviolet (UV) fluorescent silica gel (Merck 60F254) and spots were visualized by iodine vapours or irradiation with UV light (254 nm). All the chemicals were purchased from Sigma-Aldrich or Lancaster Synthesis Corporation (U.K.). Intermediates **10**–**12**, **17** and **18** were prepared according to the reported procedure [19,27,28].

4.1.1. General procedure for preparation of 13a and 13b

A mixture of compound **12** (1 g, 2.88 mmol) and benzyl bromide (0.36 mL, 2.88 mmol) or ethyl bromide (0.21 mL, 2.78 mmol) in ethanol (30 mL) containing potassium hydroxide (0.2 g, 3.57 mmol) was stirred at room temperature for 2 h. The reaction mixture was

poured onto ice water (30 mL); the separated product was filtered and crystallized from ethanol/H₂O.

4.1.2. *N*-benzyl-2-(5-(benzylthio)-1,3,4-oxadiazol-2-yl)benzenesulfonamide (13a)

Yellowish white solid, Yield: 70%; m.p.: 110–112 °C; IR: ν = 3154 (NH), 3030 (CH, aromatic), 2932 (CH, aliphatic), 1548 (C=N), 1459 (C=C), 1331 (SO₂) cm⁻¹. ¹H NMR (400 MHz, DMSO): δ = 4.11 (d, *J* = 6.6 Hz, 2H, NCH₂), 4.57 (s, 2H, S-CH₂), 7.19–7.29 (m, 5H, Ar-H), 7.28 (d, *J* = 7.2 Hz, 1H, Ar-H), 7.36 (t, *J* = 6.6 Hz, 2H, Ar-H), 7.49 (d, *J* = 8.4 Hz, 2H, Ar-H), 7.76–7.85 (m, 2H, Ar-H), 7.98–8.05 (m, 1H, Ar-H), 8.10 (t, *J* = 6.6 Hz, 1H, Ar-H), 8.30 (s, 1H, NH) ppm. ¹³C NMR (100 MHz, DMSO): δ = 35.5 (S-CH₂), 46.1 (N-CH₂), 121.4, 127.2, 127.5, 127.6, 127.8, 128.2, 128.8, 129.1, 132.1, 132.5, 136.3, 137.4, 140.3 (C=C Ar), 163.6, 164.0 (oxadiazole-C) ppm. Anal. Calcd for C₂₂H₁₉N₃O₃S₂ (437.53): C, 60.39; H, 4.38; N, 9.60; Found: C, 60.54; H, 4.55; N, 9.92%.

4.1.3. *N*-benzyl-2-(5-(ethylthio)-1,3,4-oxadiazol-2-yl)benzenesulfonamide (13b)

Yellowish white solid, Yield: 75%; m.p.: 98–100 °C; IR: ν = 3190 (NH), 3021 (CH, aromatic), 2970 (CH, aliphatic), 1550 (C=N), 1460 (C=C), 1334 (SO₂) cm⁻¹. ¹H NMR (400 MHz, DMSO): δ = 1.42 (t, *J* = 7.6 Hz, 3H, CH₃), 3.30 (q, *J* = 10.8 Hz, 2H, CH₂), 4.10 (d, *J* = 9 Hz, 2H, N-CH₂), 7.21–7.32 (m, 3H, Ar-H), 7.75–7.80 (m, 4H, Ar-H), 8.00–8.02 (m, 1H, Ar-H), 8.32–8.35 (m, 1H, Ar-H), 8.37 (s, 1H, NH) ppm. ¹³C NMR (100 MHz, DMSO): δ = 14.9 (CH₃), 26.7 (S-CH₂), 46.1 (N-CH₂), 121.5, 127.2, 127.5, 127.7, 128.2, 128.7, 132.1, 132.4, 132.5, 137.4, 140.4 (Csp²+phenyl-C), 163.4, 164.4 (oxadiazole-C) ppm. Anal. Calcd for C₁₇H₁₇N₃O₃S₂ (375.47): C, 54.38; H, 4.56; N, 11.19; Found: C, 54.41; H, 4.69; N, 11.42%.

4.1.4. Monopotassium(II) mono(2-(2-(*N*-benzylsulfamoyl)benzoyl)hydrazinecarbodithioate) (14)

Carbon disulphide (0.2 mL, 3.38 mmol) was added dropwise to cold solution of potassium hydroxide (0.3 g, 5.36 mmol) in ethanol (10 mL) containing acid hydrazide **11** (0.5 g, 1.64 mmol). The mixture was diluted with ethanol (10 mL) and stirred at room temperature for 14 h. Dry ether (20 mL) was then added and the separated solid was filtered and washed with ether (2 × 20 mL). The obtained product, in nearly quantitative yield, was employed in the next reaction without further purification.

4.1.5. 2-(4-Amino-5-mercapto-4H-1,2,4-triazol-3-yl)-*N*-benzylbenzenesulfonamide (15)

A suspension of compound **14** (0.40 g, 0.96 mmol) in hydrazine hydrate 98% (0.1 mL, 2 mmol) was heated under reflux while stirring for 1 h. Cold water (5 mL) was added and the mixture was then neutralized with concentrated 2 N hydrochloric acid (1.0 mL). The separated product was filtered, washed with cold water and crystallized from ethanol/H₂O. White solid, Yield: 60%; m.p.: 210–212 °C; IR: ν = 3289, 3200 (NH₂), 3146 (NH), 3035 (CH, aromatic), 2965 (CH, aliphatic), 1566 (C=N), 1485 (C=C), 1324 (SO₂) cm⁻¹. ¹H NMR (400 MHz, DMSO): δ = 4.08 (d, *J* = 9.6 Hz, 2H, CH₂), 4.60 (s, 2H, NH₂), 7.21–7.34 (m, 6H, Ar-H), 7.51 (d, *J* = 10.8 Hz, 1H, Ar-H), 7.61 (t, *J* = 10.2 Hz, 1H, Ar-H), 7.68 (t, *J* = 9.6 Hz, 1H, Ar-H), 7.87 (s, 1H, NH), 9.93 (s, 1H, SH) ppm. ¹³C NMR (100 MHz, DMSO): δ = 46.6 (CH₂), 127.8(0), 127.8(7), 128.1, 128.3, 129.5, 130.1, 132.5, 134.1, 137.3 (Csp²+phenyl-C), 137.8 (C=N), 167.3 (C-SH) ppm. MS: *m/z* (rel. int.) = 361 (M16.70), 209 (20.40), 241 (9.30), 295 (11.10), 123 (11.10), 106 (18.50), 91 (100.00). Anal. Calcd for C₁₅H₁₅N₅O₂S₂ (361.44): C, 49.84; H, 4.18; N, 19.38; Found: C, 49.83; H, 3.73; N, 19.59%.

4.1.6. General procedure for preparation of compounds 16a-d

A mixture of equimolar amounts of **15** (0.3 g, 0.83 mmol) and the respective aromatic aldehyde (0.83 mmol); previously dissolved separately in glacial acetic acid (1.00 mL) was heated under reflux for 20 min. The reaction mixture was cooled, diluted with water (5.00 mL) and the precipitated azomethine was filtered and then crystallized from ethanol.

4.1.7. (*E*)-*N*-((2-(4-(benzylideneamino)-5-mercapto-4H-1,2,4-triazol-3-yl)phenyl)sulfonyl)benzamide (16a)

Light yellow solid, Yield: 65%; m.p.: 207–209 °C; IR: ν = 3458 (NH), 3065 (CH, aromatic), 2977 (CH, aliphatic), 1592 (C=N), 1497 (C=C), 1327 (SO₂) cm⁻¹. ¹H NMR (400 MHz, DMSO): δ = 4.08 (s, 2H, CH₂), 7.23–7.30 (m, 8H, Ar-H), 7.64–7.63 (m, 2H, Ar-H), 7.72–7.75 (m, 3H, Ar-H), 7.96 (s, 1H, ArH), 7.98 (s, 1H, NH), 8.14 (s, 1H, CH=N), 13.14 (s, 1H, SH) ppm. ¹³C NMR (100 MHz, DMSO): δ = 46.6 (CH₂), 119.3, 127.7, 128.1, 128.7, 129.2, 129.3, 131.6, 132.9, 133.1, 138.0, 139.1, 140.4, 144.0, 147.3 (phenyl-C), 149.6, (C=N triazole), 161.7, (C=N), 172.7 (C-SH) ppm. Anal. Calcd for C₂₂H₁₉N₅O₂S₂ (449.55): C, 58.78; H, 4.26; N, 15.58; Found: C, 59.09; H, 4.35; N, 15.16%.

4.1.8. (*E*)-*N*-((2-(4-(4-chlorobenzylidene)amino)-5-mercapto-4H-1,2,4-triazol-3-yl)phenyl)sulfonyl benzamide (16b)

Light yellow solid, Yield: 60%; m.p.: 214–216 °C; IR: ν = 3182 (NH), 3040 (CH, aromatic), 2992 (CH, aliphatic), 1661 (C=N), 1588 (C=C), 1327 (SO₂) cm⁻¹. ¹H NMR (600 MHz, DMSO): δ = 4.92 (s, 2H, CH₂), 7.18–7.28 (m, 2H, Ar-H), 7.29–7.34 (m, 1H, Ar-H), 7.36 (t, *J* = 7.8 Hz, 2H, Ar-H), 7.40–7.54 (m, 3H, Ar-H), 7.86–7.93 (m, 1H, Ar-H), 7.98–8.09 (m, 2H, Ar-H), 8.10 (d, *J* = 7.8 Hz, 1H, Ar-H), 8.32 (d, *J* = 7.8 Hz, 1H, Ar-H), 8.72 (s, 1H, NH), 12.20 (s, 1H, CH=N), 13.88 (s, 1H, SH) ppm. ¹³C NMR (150 MHz, DMSO): δ = 46.0 (CH₂), 121.6, 124.1, 125.2, 126.6, 127.6, 127.8, 128.8, 128.9, 132.0, 133.7, 135.9, 136.8, 137.6, (phenyl-C), 140.9 (C=N of triazole), 158.6 (C=N), 161.4 (C-SH) ppm. MS: *m/z* (rel. int.) = 483 (M277, 13.00), 407 (10.90), + (6.50), 209 (28.30), 160 (32.50), 103 (100.00). Anal. Calcd for C₂₂H₁₈ClN₅O₂S₂ (483.99): C, 54.59; H, 3.75; N, 14.47. Found: C, 54.58; H, 3.41; N, 14.66%.

4.1.9. (*E*)-*N*-((2-(4-(4-bromobenzylidene)amino)-5-mercapto-4H-1,2,4-triazol-3-yl)phenyl)sulfonyl benzamide (16c)

Yellow solid, Yield: 70%; m.p.: 240–242 °C; IR: ν = 3428 (NH), 3036 (CH, aromatic), 2960 (CH, aliphatic), 1654 (C=N), 1551 (C=C), 1488 (C=S), 1326 (SO₂) cm⁻¹. ¹H NMR (400 MHz, DMSO): δ = 5.65 (s, 2H, CH₂), 7.50–7.64 (m, 4H, Ar-H), 7.65–7.85 (m, 5H, Ar-H), 7.96 (d, *J* = 12.6 Hz, 2H, Ar-H), 8.31 (s, 1H, Ar-H), 8.71 (s, 1H, Ar-H), 10.22 (s, 1H, NH), 10.87 (s, 1H, CH=N), 13.42 (s, 1H, SH) ppm. ¹³C NMR (100 MHz, DMSO): δ = 43.9 (CH₂), 113.9, 118.5, 118.7, 122.1, 122.2, 128.6, 128.8, 129.4, 130.6, 132.9, 133.7, 137.2, 139.3, 139.4 (phenyl-C), 155.1, (C=N triazole), 155.4 (C=N), 167.8 (C-SH) ppm. Anal. Calcd for C₂₂H₁₈BrN₅O₂S₂ (528.44): C, 50.00; H, 3.43; N, 13.25. Found: C, 49.83; H, 3.73; N, 13.24%.

4.1.10. (*E*)-*N*-((2-(5-mercapto-4-(4-methoxybenzylidene)amino)-4H-1,2,4-triazol-3-yl)phenyl)sulfonyl benzamide (16d)

Light yellow solid, Yield: 55%; m.p.: 200–202 °C; IR: ν = 3452 (NH), 3086 (CH, aromatic), 2969 (CH, aliphatic), 1596 (C=N), 1501 (C=C), 1325 (SO₂) cm⁻¹. ¹H NMR (600 MHz, DMSO): δ = 3.79 (s, 3H, OCH₃), 5.48 (s, 2H, CH₂), 6.97–7.55 (m, 13H, ArH), 8.24 (s, 1H, NH), 10.45 (s, 1H, CH=N), 12.90 (s, 1H, SH) ppm. ¹³C NMR (150 MHz, DMSO): δ = 40.0 (CH₂), 55.4 (OCH₃), 114.2, 114.4, 127.3, 127.9, 144.0, (phenyl-C), 149.7 (2C = N of triazole), 160.1 (C=N), 164.3 (C-SH) ppm. Anal. Calcd for C₂₃H₂₁N₅O₃S₂ (479.57): C, 57.60; H, 4.41; N, 14.60; Found: C, 58.00; H, 3.98; N, 14.66%.

4.1.11. General procedure for preparation of 19, 20 and 23

To a solution of the acid hydrazides **18** (0.4 g, 1.56 mmol) or **22** (0.49 g, 1.56 mmol) in ethanol (10 mL) containing glacial acetic acid (2 mL), an equimolar amount of ethylbenzoyl acetate (0.30 g, 1.56 mol) or benzoylacetone (0.25 g, 1.56 mol) was added. The reaction mixture was heated under reflux for 12 h, concentrated under reduced pressure, cooled and added to ice cold water (10 mL). The separated product was filtered, washed with water and crystallized from ethanol.

4.1.12. *N*-isopropyl-2-(5-oxo-3-phenyl-4,5-dihydro-1H-pyrazole-1-carbonyl)benzenesulfonamide (19)

White solid, Yield: 80%; m.p.: 102–104 °C; IR: $\nu = 3148$ (NH), 3061 (CH, aromatic), 2963 (CH, aliphatic), 1606 (CO), 1551 (C=N), 1502 (C=C), 1359 (SO₂) cm⁻¹. ¹H NMR (200 MHz, DMSO): $\delta = 0.93$ – 1.05 (m, 6H, 2CH₃), 1.88 – 2.15 (m, 1H, CH), 2.35 (s, 2H, CH₂), 6.72 – 7.97 (m, 10H, ArH + NH) ppm. ¹³C NMR (50 MHz, DMSO): $\delta = 24.2$ (CH₃), 39.4 (CH₂), 52.3 (CH), 122.8 , 127.6 , 127.8 , 131.9 , 132.5 , 137.7 , 135.2 , 135.4 , 138.5 , 155.6 , 163.8 , 169.4 . Anal. Calcd for C₁₉H₁₉N₃O₄S (385.44): C, 59.21; H, 4.97; N, 10.90; Found: C, 59.50; H, 5.01; N, 10.62%.

4.1.13. *N*-isopropyl-2-(3-methyl-5-phenyl-1H-pyrazole-1-carbonyl)benzenesulfonamide (20)

White solid, Yield: 85%; m.p.: 150–152 °C; IR: $\nu = 3256$ (NH), 3062 (CH, aromatic), 2973 (CH, aliphatic), 1640 (CO), 1551 (C=N), 1475 (C=C), 1321 (SO₂) cm⁻¹. ¹H NMR (400 MHz, DMSO): $\delta = 0.88$ (d, $J = 6.4$ Hz, 3H, CH₃), 0.97 (d, $J = 6.4$ Hz, 3H, CH₃), 1.88 (s, 3H, CH₃), 3.01 – 3.20 (m, 1H, CH), 6.71 (s, 1H, CH of pyrazole), 6.91 – 7.97 (m, 9H, ArH), 11.00 (s, 1H, NH) ppm. ¹³C NMR (100 MHz, DMSO): $\delta = 16.0$ (CH₃), 23.7 (2CH₃), 56.1 (CH), 92.8 (CH of pyrazole), 125.2 , 127.4 , 127.6 , 128.3 , 128.9 , 130.1 , 131.6 , 132.9 , 136.6 , 138.1 , 139.5 , 144.1 , 155.5 (phenyl-C+ pyrazole-C), 165.6 (C=O) ppm. Anal. Calcd for C₂₀H₂₁N₃O₃S (383.46): C, 62.64; H, 5.52; N, 10.96; Found: C, 63.01; H, 5.98; N, 11.33%.

4.1.14. Diethyl 2-(1,1-dioxido-3-oxobenzod[isothiazol-2(3H)-yl]malonate (21)

To a solution of saccharin sodium **2** (0.5 g, 2.44 mmol) in dimethylformamide (5 mL), diethyl 2-bromomalonate (0.6 g, 2.52 mmol) was added. The reaction was maintained at 100 °C for 2 h, then cooled and diluted with water (10 mL). The obtained product was crystallized from ethanol. White solid, Yield: 85%; m.p.: 90–92 °C; IR: $\nu = 3088$ (CH, aromatic), 2992 (CH, aliphatic), 1737 (CO, ester), 1590 (C=N), 1464 (C=C), 1332 (SO₂) cm⁻¹. ¹H NMR (400 MHz, DMSO): $\delta = 1.20$ (t, $J = 7.10$ Hz, 6H, 2CH₃), 4.14 – 4.20 (m, 4H, 2CH₂), 4.62 (s, 1H, CH), 8.02 – 8.37 (m, 4H, ArH) ppm. ¹³C NMR (100 MHz, DMSO): $\delta = 14.4$ (CH₃), 39.5 (CH₂), 62.0 (CH), 122.3 , 125.8 , 126.4 , 136.0 , 136.7 , 137.5 (phenyl-C), 159.0 , 166.8 (C=O) ppm. Anal. Calcd for C₁₄H₁₅NO₇S (341.34): C, 49.26; H, 4.43; N, 4.10. Found: C, 49.10; H, 4.30; N, 4.45%.

4.1.15. 2-(1,1-Dioxido-3-oxobenzod[isothiazol-2(3H)-yl]malonohydrazide (22)

A mixture of diester **21** (0.4 g, 1.17 mmol) and hydrazine hydrate 98% (0.5 mL, 10.00 mmol) was stirred at room temperature for 20 min. The separated product was filtered, washed with water, dried and crystallized from ethanol. White solid, Yield: 80%; m.p.: 100–102 °C; IR: $\nu = 3385$, 3331 (2NH), 3289 , 3190 (2NH₂), 3097 (CH, aromatic), 1665 , 1619 (CO), 1507 (C=C), 1333 (SO₂) cm⁻¹. ¹H NMR (400 MHz, DMSO): $\delta = 3.80$ (s, 1H, CH), 4.35 (br s, 4H, 2NH₂, exch.), 7.51 – 7.88 (m, 4H, ArH), 9.12 (s, 1H, NH, exch.), 9.89 (s, 1H, NH, exch.) ppm. ¹³C NMR (100 MHz, DMSO): $\delta = 44.07$ (CH), 128.7 , 129.6 , 130.1 , 132.8 , 134.3 , 137.0 (phenyl-C), 166.5 , 167.0 , 170.9 (3C=O) ppm. Anal. Calcd for C₁₀H₁₁N₅O₅S (313.29): C, 38.34; H, 3.54; N, 22.35. Found: C, 38.10; H, 3.30; N, 21.90%.

4.1.16. 2-(1,1-Dioxido-3-oxobenzod[isothiazol-2(3H)-yl]-1,3-bis(3-methyl-5-phenyl-1H-pyrazol-1-yl)propane-1,3-dione (23)

White solid, Yield: 75%; m.p.: 160–162 °C; crystallized from ethanol; IR: $\nu = 3076$ (CH, aromatic), 2965 (CH, aliphatic), 1734 , 1665 (CO), 1580 (C=N), 1505 (C=C), 1332 (SO₂) cm⁻¹. ¹H NMR (400 MHz, DMSO): $\delta = 2.25$ (s, 6H, 2CH₃), 5.48 (s, 1H, CH), 6.44 (s, 2H, 2CH of pyrazole), 7.27 (t, $J = 11.4$ Hz, 2H, Ar-H), 7.39 (t, $J = 11.4$ Hz, 6H, Ar-H), 7.74 (d, $J = 11.4$ Hz, 6H, Ar-H) ppm. ¹³C NMR (100 MHz, DMSO): $\delta = 10.6$ (2CH₃), 40.1 (CH), 101.1 (2CH of pyrazole), 121.7 , 124.6 , 124.9 , 125.1 , 126.4 , 127.2 , 128.6 , 132.7 , 135.3 , 135.9 , 136.9 , 139.4 , 150.4 (phenyl-C+ pyrazole-C), 158.5 , 158.6 , 163.4 (3C=O) ppm. Anal. Calcd for C₃₀H₂₃N₅O₅S (565.60): C, 63.71; H, 4.10; N, 12.38; Found: C, 64.05; H, 4.49; N, 11.94%.

4.1.17. General procedure for preparation of 24a-c

A mixture of equimolar amounts of the dihydrazide **22** (0.49 g, 1.56 mmol) and the appropriate aromatic aldehydes (1.56 mmol) in ethanol (10 mL) containing glacial acetic acid (2 mL) was heated under reflux for 2 h. The reaction mixture was cooled and the separated product was filtered, washed with water (10 mL), dried and crystallized from ethanol.

4.1.18. *N*¹,*N*³-di((*E*)-benzylidene)-2-(1,1-dioxido-3-oxobenzod[isothiazol-2(3H)-yl]malonohydrazide (24a)

White solid, Yield: 75%; m.p.: 120–122 °C; IR: $\nu = 3450$, 3241 (2NH), 3062 (CH, aromatic), 2951 (CH, aliphatic), 1749 , 1672 (CO), 1496 (C=C), 1334 (SO₂) cm⁻¹. ¹H NMR (600 MHz, DMSO): $\delta = 4.19$ (s, 1H, CH-N), 7.29 – 8.00 (m, 14H, ArH), 8.29 (s, 1H, CH=N), 8.30 (s, 1H, CH=N), 11.39 (s, 1H, NH), 12.08 (s, 1H, NH) ppm. ¹³C NMR (150 MHz, DMSO): $\delta = 79.3$ (CH-N), 126.5 , 126.9 , 127.2 , 128.1 , 128.35 , 128.7 , 128.9 , 129.2 , 129.4 , 129.7 , 129.9 , 130.0 , 130.1 , 130.3 , 130.4 , 132.0 , 137.9 , 143.8 , 144.1 (phenyl C), 148.2 , 148.4 (2C=N), 163.9 , 165.7 , 169.0 (3C=O) ppm. Anal. Calcd for C₂₄H₁₉N₅O₅S (489.50): C, 58.89; H, 3.91; N, 14.31; Found: C, 58.58; H, 3.64; N, 14.10%.

4.1.19. 2-(1,1-Dioxido-3-oxobenzod[isothiazol-2(3H)-yl]-*N*¹,*N*³-bis((*E*)-4-fluorobenzylidene)malono-hydrazide (24b)

White solid, Yield: 85%; m.p.: 116–118 °C; IR: $\nu = 3460$, 3181 (2NH), 3096 (CH, aromatic), 2953 (CH, aliphatic), 1746 , 1680 , 1628 (CO), 1460 (C=C), 1331 (SO₂) cm⁻¹. ¹H NMR (400 MHz, DMSO): $\delta = 4.93$ (s, 1H, CH-N), 7.29 (t, $J = 13.2$ Hz, 2H, Ar-H), 7.69 – 7.92 (m, 3H, Ar-H), 7.97 – 8.29 (m, 7H, Ar-H), 8.36 (d, $J = 10.8$ Hz, 2H, 2CH=N), 11.76 (s, 1H, NH), 11.83 (s, 1H, NH) ppm. ¹³C NMR (100 MHz, DMSO): $\delta = 78.7$ (CH-N), 116.2 , 116.3 , 116.4 , 122.2 , 125.6 , 125.7 , 126.8 , 126.9 , 129.8 , 129.9 , 131.0 , 135.8 , 136.5 , 137.6 , 143.9 (phenyl-C), 147.0 , 159.2 (2C=N), 161.8 (phenyl-C-F), 162.4 , 164.8 , 166.2 (3C=O) ppm. Anal. Calcd for C₂₄H₁₇F₂N₅O₅S (525.48): C, 54.86; H, 3.26; N, 13.20. Found: C, 54.58; H, 3.41; N, 13.20%.

4.1.20. 2-Methyl-di-(4-chlorobenzylidenehydrazinocarbonyl)-1,2-benzisothiazole-3(2H)-one-1,1-dioxide (24c)

White solid, Yield: 70%; m.p.: 130–132 °C; IR: $\nu = 3461$, 3182 (2NH), 3088 (CH, aromatic), 2951 (CH, aliphatic), 1745 , 1679 (CO), 1497 (C=C), 1330 (SO₂) cm⁻¹. ¹H NMR (400 MHz, DMSO): $\delta = 4.93$ (s, 1H, CH-N), 7.50 (d, $J = 12.6$ Hz, 2H, Ar-H), 7.74 (d, $J = 12.6$ Hz, 1H, Ar-H), 7.80 (d, $J = 12.6$ Hz, 2H, Ar-H), 7.97 – 8.26 (m, 6H, Ar-H), 8.36 (d, $J = 12.6$ Hz, 1H, Ar-H), 8.72 (s, 2H, 2CH=N), 11.83 (s, 1H, NH), 11.89 (s, 1H, NH) ppm. ¹³C NMR (100 MHz, DMSO): $\delta = 83.2$ (CH-N), 121.8 , 125.2 , 126.3 , 128 (8), 128.9 , 129.1 , 130.0 , 132.8 , 132.9 , 134.6 , 135.4 , 136.0 , 136.9 , 137.1 (phenyl-C), 143.3 , 146.4 (C=N), 158.8 , 161.5 , 165.8 (3C=O) ppm. Anal. Calcd for C₂₄H₁₇Cl₂N₅O₅S (558.39): C, 51.62; H, 3.07; N, 12.54; Found: C, 51.32; H, 3.36; N, 12.31%.

4.2. Biology

4.2.1. *In vitro* COX-1/COX-2 enzyme inhibition assay

The synthesized compounds **12–13a-b**, **16a-d**, **19**, **20**, **23–24a-c** were tested for their ability to inhibit COX-1 and/or COX-2 enzymes using Cayman's colorimetric COX (ovine) assay and the results were recorded in Table 1. The assay measures the peroxidase activity colorimetrically by monitoring the appearance of oxidized *N,N,N',N'*-tetramethyl-*p*-phenylenediamine at 590 nm as reported by Kulmacz and Lands [29].

4.2.2. *In vivo* assay

4.2.2.1. Materials. Carrageenan (carrageenan kappa-type III) and all other reagents were purchased from Sigma Chemical Co. (St. Louis, MO, USA). The test compounds **15**, **19**, **20**, **23**, **24b** and reference drugs celecoxib and/or indomethacin were used in the following assays. Housing and management of the animals and the experimental protocols were made as stipulated in the Guide for Care and Use of Laboratory Animals Guidelines of the National Institutes of Health (NIH), and accepted by the local authorities of Zagazig University, Zagazig, Egypt.

4.2.2.2. Animals. Mature male albino rats weighing 150–200 g were used. All experimental animals were provided from the Faculty of Veterinary Medicine, Zagazig University, Egypt. All animals were held under standard laboratory conditions in the animal house (temperature 27 °C) with a 12/12 light-dark cycle. Animals were fed laboratory diet and water ad libitum. All experiments were carried out using six animals per group. The animal experiments were performed in accordance with international guidelines.

4.2.2.3. Anti-inflammatory effect evaluation. The rat hind paw edema method by Winter et al., 1962 [30] was applied to determine the anti-inflammatory activity of the test compounds **15**, **19**, **20**, **23** and **24b** using celecoxib as a standard. Mature male albino rats weighing 150–200 g was used. The animals were divided into 7 equal groups (each of six). The first group was left as a control group while the second group was injected i.p. with celecoxib at a dose of 18 mg/kg body weight. The test compounds were injected i.p. in the remaining groups at the same dose level. After 1 h, edema in the right hind paw was induced by injecting 0.1 mL of 10% carrageenin. The thickness of the paw was measured using a skin caliber 1, 2, 3, and 4 h after the carrageenin injection to determine the anti-inflammatory activity of the test compounds (Table 2).

4.2.2.4. Ulcerogenic liability. The compounds **15**, **19**, **20**, **23** and **24b** were tested for their ulcerogenic activity using celecoxib and indomethacin as reference drugs [22]. Male albino rats weighing 150–200 g were fasted for 12 h prior to drug administration. Water was given ad libitum. The animals were divided into eight equal groups (each of six). The first group was received 1% gum acacia (suspending vehicle) orally once a day and left as a control while the second group was received celecoxib at a dose of 18 mg/kg/day orally. The third group was received indomethacin at a dose of 18 mg/kg/day orally. The remaining groups were received the test compounds at a dose of 18 mg/kg/day orally. The drugs were administered orally once a day for three successive days. Animals were sacrificed by over dosage of ether after 6 h from the last dose. The stomach was removed, opened along the greater curvature and examined for ulceration. The number and severity of discrete areas of damage in the glandular mucosa were scored (Table 3). The ulcer score was calculated according to the 1 to 5 scoring system devised by Wilhelmi and Menasse-Gdynia [22] (Table 3). Stomach ulceration was expressed in terms of ulcer index (U.I.) Ulcer index (U.I.) = mean

ulcer score of a group of animals similarly treated × % of ulcerated animals of this group [31].

Ulcer score:

1: 1 or 2-min sporadic punctate lesions, 2: Several small lesions, 3: One extensive lesion or multiple moderate-sized lesions, 4: Several large lesions, 5: Several large lesions with stomach perforation.

4.2.3. Docking

The molecular docking of the tested compounds **19**, **20** and **23** was performed using Molecular Operating Environment software utilizing the reported protein crystallographic structure of COX-2 (PDB code: 3ln1). Celecoxib was the crystallized ligand into the COX-2 protein active site. The tested structures were created using ChemDraw professional (version: 15.1.0.144) and were energy minimized using the MMF94X forcefield to a constant of 0.05 kcal/mol. The protein was prepared for docking process with removing the water and adding the polar hydrogens. Standard Docking of **19**, **20** and **23** and celecoxib into the active site of the COX-2 was performed using the standard docking function in MOE. Firstly, docking was restricted at the active site, however, compound **23** did not fit into the active site, may be due to bulky side groups, so docking against other pockets was performed. The top 30 docking poses finally saved and were ranked according to their interaction energy and examined for fit and possible interactions with the active site.

Acknowledgment

The authors are kindly appreciative to "Patrick McCosker at School of Chemistry, University of Wollongong, for his efforts proofreading the Manuscript." Dr Naglaa Z. Eleiwa, Zagazig University, Faculty of veterinary medicine is highly appreciated for her kind co-operation in carrying out the experimental biological part.

Appendix A. Supplementary data

Supplementary data to this article can be found online at <https://doi.org/10.1016/j.ejmech.2019.03.042>.

References

- [1] G. Onder, F. Pellicciotti, G. Gambass, R. Bernabei, NSAID-related psychiatric adverse events: who is at risk? *Drugs* 64 (2004) 2619–2627, <https://doi.org/10.2165/00003495-200464230-00001>.
- [2] S.P. Khanapure, D.S. Garvey, D.V. Young, M. Ezawa, R.A. Earl, R.D. Gaston, X. Fang, M. Murty, A. Martino, M. Shumway, M. Trocha, P. Marek, S.W. Tam, D.R. Janero, L.G. Letts, Synthesis and structure-activity relationship of novel, highly potent methyl and methycycloalkyl cyclooxygenase-2 (COX-2) selective inhibitors, *J. Med. Chem.* 46 (2003) 5484–5504, <https://doi.org/10.1021/jm030268b>.
- [3] R. Bai, J. Sun, Z. Liang, Y. Yoon, E. Salgado, A. Feng, Y. Oum, Y. Xie, H. Shim, Anti-inflammatory hybrids of secondary amines and amide-sulfamide derivatives, *Eur. J. Med. Chem.* 150 (2018) 195–205, <https://doi.org/10.1016/j.ejmech.2018.02.085>.
- [4] C. Johnson-Mann, K. Rawlings, R.A. Arbizu, A. Hebra, NSAID induced perforated peptic ulcer in a pediatric sickle cell patient, *J. Pediatr. Case Reports*. 14 (2016) 12–14, <https://doi.org/10.1016/j.epsc.2016.08.005>.
- [5] J.A. Cairn, The coxibs and traditional nonsteroidal anti-inflammatory drugs: a current perspective on cardiovascular risks, *Can. J. Cardiol.* 23 (2007) 125–131, [https://doi.org/10.1016/S0828-282X\(07\)70732-8](https://doi.org/10.1016/S0828-282X(07)70732-8).
- [6] G. Bozimoski, A review of nonsteroidal anti-inflammatory drugs, *AANA J. (Am. Assoc. Nurse Anesth.)* 83 (2015) 425–433.
- [7] C. Pereira-Leite, C. Nunes, S.K. Jamal, I.M. Cuccovia, S. Reis, Nonsteroidal anti-inflammatory therapy: a journey toward safety, *Med. Res. Rev.* 37 (2017) 802–859, <https://doi.org/10.1002/med.21424>.
- [8] S.K. Suthar, M. Sharma, Recent developments in chimeric NSAIDs as safer anti-inflammatory agents, *Med. Res. Rev.* 35 (2015) 341–407, <https://doi.org/10.1002/med.21331>.
- [9] G.S. Hassan, S.M. Abou-Seri, G. Kamel, M.M. Ali, Celecoxib analogs bearing benzofuran moiety as cyclooxygenase-2 inhibitors: design, synthesis and evaluation as potential anti-inflammatory agents, *Eur. J. Med. Chem.* 76 (2014) 482–493, <https://doi.org/10.1016/j.ejmech.2014.02.033>.

- [10] S. Zhou, S. Yang, G. Huang, Design, synthesis and bioactivities of Celecoxib analogues or derivatives, *Bioorg. Med. Chem.* 25 (2017) 4887–4893, <https://doi.org/10.1016/j.bmc.2017.07.038>.
- [11] S.P. Chavan, K. Adithyraj, B.M. Bhanage, In situ generation and utilization of CO: an efficient route towards N-substituted saccharin via carbonylative cyclization of 2-iodosulfonamides, *Synlett* 28 (2017) 2000–2003, <https://doi.org/10.1055/s-0036-1588422>.
- [12] S. Xu, C.A. Rouzer, L.J. Marnett, Oxycams, a class of NSAIDs and beyond, *IUBMB Life* 66 (2014) 803–811, <https://doi.org/10.1002/iub.1334>.
- [13] E.H. Abdel Aal, O.I. El-Sabbagh, S. Youssif, S.M. El-Nabtity, Synthesis and some pharmacological studies of new benzenesulfonamide derivatives, *Monatsh. Chem.* 133 (2002) 255–266.
- [14] O.I. El-Sabbagh, S.M. Ibrahim, M.M. Baraka, H. Kothayer, Synthesis of new 2,3-dihydroquinazolin-4(1H)-one derivatives for analgesic and anti-inflammatory evaluation, *Arch. Pharm. (Weinheim)* 343 (2010) 274–281, <https://doi.org/10.1002/ardp.200900220>.
- [15] M.A. El-Sayed, N.I. Abdel-Aziz, A.A.-M. Abdel-Aziz, A.S. El-Azab, Y.A. Asiri, K.E.H. ElTahir, Design, synthesis, and biological evaluation of substituted hydrazone and pyrazole derivatives as selective COX-2 inhibitors: molecular docking study, *Bioorg. Med. Chem.* 19 (2011) 3416–3424, <https://doi.org/10.1016/j.bmc.2011.04.027>.
- [16] S. Ovais, S. Yaseen, R. Bashir, P. Rathore, M. Samim, S. Singh, V. Nair, K. Javed, Synthesis and anti-inflammatory activity of celecoxib like compounds, *J. Enzym. Inhib. Med. Chem.* 28 (2013) 1105–1112, <https://doi.org/10.3109/14756366.2012.710847>.
- [17] H.A. Abdel-Aziz, K.A. Al-Rashood, K.E.H. ElTahir, G.M. Suddek, Synthesis of N-benzenesulfonamide-1H-pyrazoles bearing arylsulfonyl moiety: novel celecoxib analogs as potent anti-inflammatory agents, *Eur. J. Med. Chem.* 80 (2010) 416–422, <https://doi.org/10.1016/j.ejmech.2014.04.065>.
- [18] H.M.A. Ashour, I.M. El-Ashmawy, A.E. Bayad, Synthesis and pharmacological evaluation of new pyrazolyl benzenesulfonamides linked to polysubstituted pyrazoles and thiazolidinones as anti-inflammatory and analgesic agents, *Monatsh. Chem.* 147 (2016) 605–618, <https://doi.org/10.1007/s00706-015-1549-x>.
- [19] O.I. El-Sabbagh, Synthesis of some new benzisothiazolone and benzenesulfonamide derivatives of biological interest starting from saccharin sodium, *Arch. Pharm. (Weinheim)* 346 (2013) 733–742, <https://doi.org/10.1002/ardp.201300110>.
- [20] K.M. Amin, M.M. Kamel, M.M. Anwar, M. Khedr, Y.M. Syam, Synthesis, biological evaluation and molecular docking of novel series of spiro [(2H,3H)-quinazoline-2,1'-cyclohexan]-4(1H)-one derivatives as anti-inflammatory and analgesic agents, *Eur. J. Med. Chem.* 45 (2010) 2117–2131, <https://doi.org/10.1016/j.ejmech.2009.12.078>.
- [21] C.A. Winter, L. Flataker, Reaction thresholds to pressure in edematous hind-paws of rats and responses to analgesic drugs, *J. Pharmacol. Exp. Ther.* 150 (1965) 165–171, <http://jpet.aspetjournals.org/content/150/1/165.long>.
- [22] G. Wilhelmi, R. Menassé-Gdynia, Gastric mucosal damage induced by non-steroid anti-inflammatory agents in rats of different ages, *Pharmacology* 8 (1972) 321–328, <https://doi.org/10.1159/000136348>.
- [23] J.L. Wang, J. Carter, J.R. Kiefer, R.G. Kurumbail, J.L. Pawlitz, D. Brown, S.J. Hartmann, M.J. Graneto, K. Seibert, J.J. Talley, The novel benzopyran class of selective cyclooxygenase-2 inhibitors-part I: the first clinical candidate, *Bioorg. Med. Chem. Lett.* 20 (2010) 7155–7158, <https://doi.org/10.1016/j.bmcl.2010.07.053>.
- [24] <http://molsoft.com/mprop/>.
- [25] M.J. Ahsan, J.G. Samy, H. Khalilullah, M.S. Nomani, P. Saraswat, R. Gaur, A. Singh, Molecular properties prediction and synthesis of novel 1,3,4-oxadiazole analogues as potent antimicrobial and antitubercular agents, *Bioorg. Med. Chem. Lett.* 21 (2011) 7246–7250, <https://doi.org/10.1016/j.bmcl.2011.10.057>.
- [26] D.F. Veber, S.R. Johnson, H.-Y. Cheng, B.R. Smith, K.W. Ward, K.D. Kopple, Molecular properties that influence the oral bioavailability of drug candidates, *J. Med. Chem.* 45 (2002) 2615–2623, <https://doi.org/10.1021/jm020017n>.
- [27] J. Ivanova, F. Carta, D. Vullo, J. Leitans, A. Kazaks, K. Tars, R. Zalubovskis, C.T. Supuran, N-Substituted and ring opened saccharin derivatives selectively inhibit transmembrane, tumor-associated carbonic anhydrases IX and XII, *Bioorg. Med. Chem.* 25 (2017) 3583–3589, <https://doi.org/10.1016/j.bmc.2017.04.007>.
- [28] A.W. Naser, A.M. Majeed, Synthesis of some new sulfonamide derivatives based on 1,3,4-oxadiazole, *J. Chem. Pharm. Res.* 7 (2015) 300–306, <https://pdfs.semanticscholar.org/5442/86d44a27d5c4367d70be10a3e5dc66282747.pdf>.
- [29] R.J. Kulmacz, W.E.M. Lands, Requirements for hydroperoxide by the cyclooxygenase and peroxidase activities of prostaglandin H synthase, *Prostaglandins* 25 (1983) 531–540, [https://doi.org/10.1016/0090-6980\(83\)90025-4](https://doi.org/10.1016/0090-6980(83)90025-4).
- [30] C.A. Winter, E.A. Risley, G.W. Nuss, Carrageenin-induced edema in hind paw of the rat as an assay for antiinflammatory drugs, *Proc. Soc. Exp. Biol. Med.* 111 (1962) 544–547, <https://doi.org/10.3181/00379727-111-27849>.
- [31] F. Paull, A.N. Wick, E.M. Mackay, An assay method for anti-ulcer substances, *Gastroenterology* 8 (1947) 774–782.